

Italian Physical Society

Proceedings of the
International School of Physics

"Enrico Fermi"

XVII COURSE

edited by A. GOZZINI

Director of the Course

VARENNA ON LAKE COMO

VILLA MONASTERO

1-17 AUGUST 1960

Topics on Radiofrequency Spectroscopy



SOCIETÀ ITALIANA DI FISICA

RENDICONTI
DELLA
SCUOLA INTERNAZIONALE DI FISICA
« ENRICO FERMI »

XVII CORSO

a cura di A. GOZZINI

Direttore del Corso

VARENNA SUL LAGO DI COMO

VILLA MONASTERO

1-17 AGOSTO 1960

Argomenti di Spettroscopia a Radiofrequenza



ACADEMIC PRESS • NEW YORK AND LONDON

ACADEMIC PRESS INC.
111 FIFTH AVENUE
NEW YORK 3, N. Y.

United Kingdom Edition

Published by
ACADEMIC PRESS INC. (LONDON) LTD.
BERKELEY SQUARE HOUSE, LONDON W. 1

COPYRIGHT © 1962, BY SOCIETÀ ITALIANA DI FISICA

ALL RIGHTS RESERVED

NO PART OF THIS BOOK MAY BE REPRODUCED IN ANY FORM,
BY PHOTOSTAT, MICROFILM, OR ANY OTHER MEANS,
WITHOUT WRITTEN PERMISSION FROM THE PUBLISHERS.

Library of Congress Catalog Card Number: 62-13643

PRINTED IN ITALY

Prolusione del Corso.

A. GOZZINI

Direttore del Corso

Benchè la nascita della Spettroscopia a Radiofrequenze coincida praticamente con quella delle onde hertziane, difficoltà di natura soprattutto tecnica ne hanno limitato per molto tempo lo sviluppo, cosicchè può dirsi che essa sia sorta negli anni immediatamente precedenti la seconda guerra mondiale, con i metodi di risonanza introdotti da RABI.

Negli anni seguenti la fine della guerra, quando le tecniche sviluppate per la realizzazione del Radar hanno potuto essere applicate alla ricerca fondamentale, questa disciplina si è sviluppata in modo vertiginoso, e la sua suddivisione iniziale nei capitoli della Spettroscopia a Microonde dei gas, e della Risonanza magnetica, ha presto perso significato.

Con Spettroscopia a radiofrequenze si designa oggi un complesso di metodi e tecniche che trovano vaste applicazioni nei campi più diversi, dalle particelle elementari alla Fisica dello stato solido, dallo studio dei sistemi isolati a quello delle proprietà dielettriche e magnetiche della materia, alla Radioastronomia, alla teoria del legame chimico.

In conseguenza, sebbene questo che inizia oggi sia il primo corso che la Scuola di Varenna dedica ufficialmente alla Spettroscopia hertziana, molti capitoli di essa sono già stati trattati in corsi precedenti. In particolare il corso sulle proprietà magnetiche della materia, organizzato dal prof. GIULOTTO nel 1956, trattò per la maggior parte i fenomeni di risonanza magnetica, elettronica e nucleare.

Negli ultimi anni, quando ormai la perfezione raggiunta dalle tecniche tradizionali e la mole del lavoro svolto lasciavano prevedere prossimo un processo di saturazione, alcune eleganti idee hanno aperto nuovi orizzonti e nuove prospettive dando un rinnovato impulso alla nostra disciplina.

Alludo al Maser, ai metodi ottici della risonanza magnetica, alle tecniche di doppia irradiazione. A tali argomenti appunto è dedicato il nostro corso, e mi è parso anche opportuno che una serie di lezioni vertesse sulle ricerche attuali condotte con le tecniche dei fasci atomici, cioè con i metodi di Rabi, tutt'oggi insostituibili nello studio degli elementi pesanti.

Molti fra coloro che queste nuove idee hanno concepito e sviluppato hanno accettato di collaborare al corso, in qualità di docenti. Ad essi esprimo, sicuro di interpretare il sentimento di tutti gli ospiti della Scuola, la più viva gratitudine ed il più commosso ringraziamento. La loro presenza e partecipazione al corso è garanzia della migliore riuscita di esso.

INDICE

A. GOZZINI - Prolusione al Corso	pag. VII
Gruppo fotografico dei partecipanti al Corso	fuori testo
K. SHIMODA - Maser spectroscopy	pag. 1
C. H. TOWNES - Masers	» 39
B. ELSCHNER - Maser à trois niveaux dans les solides	» 68
J. DE PRINS et P. KARTASCHOFF - Applications de la spectroscopie hertzienne à la mesure des fréquences et du temps	» 88
R. A. MARRUS and W. A. NIERENBERG - On atomic beams	» 118
A. KASTLER - Spectroscopie à radiofréquence dans les atomes optiquement orientés	» 157
J. BROSSEL - Les méthodes optiques de la résonance magnétique	» 187
T. SKALIŃSKI - Les diverses méthodes de pompage et détection optique et leurs applications à l'étude des états fondamentaux de métaux alcalins	» 212
C. COHEN-TANNOUDJI - Phénomènes de cohérence en résonance optique	» 240
A. D. MAY - Radio frequency spectroscopy. Magnetic resonance of several atomic levels of Zn I, Zn II and of Cd II excited by electronic bombardment	» 254
J. WINTER - Résonance à plusieurs quanta	» 259
A. DI GIACOMO - Transitions dipolaires électriques à deux quanta dans les gaz	» 273
A. ABRAGAM - Les méthodes de double irradiation en résonance magnétique dans les liquides et les solides	» 281
CH. RYTER - Mesure directe de la densité électronique à l'emplacement du noyau de lithium métallique	» 303
C. ROBERT et J. M. WINTER - Résonance nucléaire dans les substances ferromagnétiques	» 308

Maser spectroscopy.

K. SHIMODA

Department of Physics, Faculty of Science, University - Tokyo

I. - Introduction.

1. - Spectroscopy of molecules, atoms and nuclei.

The angular momentum of a quantum-mechanical system has the magnitude of the order of \hbar . But the moment of inertia has different order of magnitudes for various cases. The moment of inertia of a molecule is given by

$$I \approx Mr^2,$$

where M is the mass of an atom, r the interatomic distance. Then the rotational energy of a molecule is

$$(1.1) \quad W_{\text{rot}} \approx \frac{\hbar^2}{Mr^2}.$$

Since the molecular force constant is of the order of e^2/r^3 , the vibrational energy of a molecule may be expressed in the form

$$(1.2) \quad W_{\text{vib}} \approx \frac{\hbar^2}{\sqrt{mMr^2}},$$

where m is the electron mass and $r \approx a_0 = \hbar^2/me^2$. The electronic energy of an atom or a molecule may be written in the form

$$(1.3) \quad W_{\text{el}} \approx \frac{\hbar^2}{mr^2}.$$

The γ -ray from a nucleus is radiated by the movement of the charge inside the

nucleus with radius R , and the nuclear excitation energy may be given by

$$(1.4) \quad W_N \approx \frac{\hbar^2}{M_p R^2},$$

where M_p is the proton mass.

Inserting the following values, $\hbar = 10^{-27}$ erg·s, $r = 10^{-8}$ cm, $R = 10^{-13}$ cm, $M = 10^{-22}$ g, $m = 10^{-27}$ g, we obtain

$$(1.1a) \quad W_{\text{rot}}/\hbar \approx 10^{11} \text{ s}^{-1}, \quad \lambda_{\text{rot}} \approx 2 \text{ mm};$$

$$(1.2a) \quad W_{\text{vib}}/\hbar \approx 3 \cdot 10^{13} \text{ s}^{-1}, \quad \lambda_{\text{vib}} \approx 60 \text{ } \mu\text{m};$$

$$(1.3a) \quad W_{\text{el}}/\hbar \approx 10^{16} \text{ s}^{-1}, \quad \lambda_{\text{el}} \approx 200 \text{ nm};$$

$$(1.4a) \quad W_N/\hbar \approx 10^{21} \text{ s}^{-1}, \quad \lambda_N \approx 0.02 \text{ } \text{\AA}.$$

These are the typical transition frequencies and wavelengths. Actual transitions generally occur at frequencies which may be two orders of magnitude higher or lower.

Because of the finite size of the nucleus, the electronic energy of an atom may be expanded in the form

$$W \approx \frac{\hbar^2}{mr^2} \left\{ 1 + 0 \left(\frac{R^2}{r^2} \right) + 0 \left(\frac{R^4}{r^4} \right) + \dots \right\},$$

where r is the distance of an electron from the center of the nucleus. The second term exhibits the quadrupole hyperfine structure which is not zero, when the nuclear spin $I \geq 1$. Since $R^2/r^2 \approx 10^{-10}$, the energy of the quadrupole hyperfine structure is

$$(1.5) \quad \frac{W_q}{\hbar} \approx \frac{\hbar}{mr^2} \frac{R^2}{r} \approx 10^6 \text{ s}^{-1}.$$

W_q is usually written as eqQ , where $Q \approx R^2$, $q \approx e/r^3$.

The third term which appears, when $I \geq 2$, represents the hexadecapole hyperfine structure.

$$(1.6) \quad \frac{W_{\text{Hd}}}{\hbar} \approx \frac{\hbar}{mr^2} \frac{R^4}{r^4} \approx 10^{-4} \text{ s}^{-1}.$$

The hexadecapole energy is so small that only one case with exceptionally large hexadecapole effect has been studied. For an atom with nucleus of larger spin, higher order interactions should occur in principle, but they are too small to be observed.

There are also magnetic interactions between electrons and nuclei. The magnetic moment of an electron is close to one Bohr magneton, $\mu_B = 0.927 \cdot 10^{-20}$ cgs, and that of an nucleus is of the order of the nuclear magneton, $\mu_N = 5.05 \cdot 10^{-24}$ cgs. The energy for the atomic fine structure is the magnetic dipole interaction energy between electrons. Since $r^{-3} \approx 10^{28} \text{ cm}^{-3}$, the frequency of fine structure is

$$(1.7) \quad \frac{W_{ee}}{\hbar} \approx \frac{\mu_B^2}{r^3 \hbar} \approx 10^{13} \text{ s}^{-1}.$$

The magnetic dipole interaction between electron and nucleus gives the hyperfine structure, which appears when $I \geq \frac{1}{2}$.

$$(1.8) \quad \frac{W_{eN}}{\hbar} \approx \frac{\mu_B \mu_N}{r^3 \hbar} \approx 5 \times 10^9 \text{ s}^{-1}.$$

The magnetic dipole interaction between nuclei in a molecule gives the so-called magnetic hyperfine structure. The distance between nuclei is $r \approx 10^{-8} \text{ cm}$, and it gives

$$(1.9) \quad \frac{W_{NN}}{\hbar} \approx \frac{\mu_N^2}{r^3 \hbar} \approx 2 \times 10^4 \text{ s}^{-1}.$$

The second higher order magnetic interaction between electron and nucleus is the magnetic octupole coupling which appears when $I \geq \frac{3}{2}$.

$$(1.10) \quad \frac{W_{\text{oct}}}{\hbar} \approx \frac{\mu_B \mu_N}{r^3 \hbar} \frac{R^2}{r^2} \approx 5 \times 10^{-1} \text{ s}^{-1}.$$

The magnetic octupole interaction has been observed for Ga, In, and I. Much higher order interaction such as 32-pole interaction for $I \geq \frac{5}{2}$ should be very small and negligible.

Equations from (1.1) to (1.10) show various types of the spectrum of molecules, atoms, and nuclei without external field. Under the magnetic field of several thousand oersted, the nuclear magnetic moment has the energy corresponding to the transition frequency of about 10 MHz. This is the so-called nuclear magnetic resonance,

$$(1.11) \quad W_{\text{NMR}} = \mu_N H.$$

Here H is the magnetic field.

The electron spin resonance is expressed by

$$(1.12) \quad W_{\text{ESR}} \approx \mu_B H.$$

Since μ_B is about 2 000 times, larger than μ_N , the frequency of the ESR transition is found in the microwave range in the magnetic field of the order of 10^4 oersteds.

2. - Sensitivity of radiofrequency and microwave spectrometers.

In order to set up a high sensitivity spectrometer, theoretical considerations of the sensitivity are quite helpful for experimental physicists. The waveguide cell or the cavity cell of the spectrometer is fed by the input power P_i , and gives the output P . At the presence of emission or absorption by molecules in the cell, the output power becomes $P + \Delta P$ and the amplitude changes from V to $V + \Delta V$.

It is not correct to assume that the spectrum is detectable when ΔP is larger than the noise power $FkT\Delta f$, because the noise figure, F , of the detector is defined for a heterodyne detection [1]. We have

$$P + \Delta P = K(V + \Delta V)^2 \simeq KV^2 + 2KV\Delta V$$

and

$$(\Delta P)^2 \simeq 4PK(\Delta V)^2.$$

Since the modulation amplitude due to molecules in the cell (*) is $\frac{1}{2}\Delta V$, the signal power which can be compared with noise should be

$$K\left(\frac{\Delta V}{2}\right)^2 = \frac{(\Delta P)^2}{16P}.$$

Then the signal may be considered detectable when

$$(2.1) \quad \frac{(\Delta P)^2}{16P} \geq FkT\Delta f,$$

where Δf is the effective bandwidth. When the image noise is taken into account, the bandwidth must be multiplied by 2, while if the phase of the signal

(*) For sinusoidal molecular modulation, at a frequency $\omega_m/2\pi$, the amplitude may be expressed in the form

$$V(t) = V \cos \omega t + \frac{\Delta V}{2} \cos (\omega + \omega_m)t,$$

where the first term corresponds to the local oscillation and the second term to the signal.

is known, it may be divided by 2, since the out-of-phase component can essentially be eliminated.

Three types of spectrometers are considered in the following.

i) *Waveguide cell.* — The change of output power from a waveguide absorption cell of length l is given by

$$(2.2) \quad \Delta P = P(\exp[-\alpha_g l] - 1) \simeq -P\alpha_g l,$$

where α_g is the absorption coefficient of the gas in the cell. Then the minimum detectable absorption is from (2.1) and (2.2)

$$(2.3) \quad \alpha_{g,\min} = \frac{4}{l} \sqrt{\frac{FkT\Delta f}{P}} = \frac{4}{l} \sqrt{\frac{FkT\Delta f}{P_i \exp[-\alpha_c l]}},$$

where α_c is the waveguide absorption coefficient. Equation (2.3) takes a minimum value for a given input power, when the cell length is

$$(2.4) \quad l_{\text{opt}} = \frac{2}{\alpha_c}.$$

The optimum value of the minimum detectable absorption coefficient for $l = l_{\text{opt}}$ is

$$(2.5) \quad \alpha_{g,\text{opt}} = 2e\alpha_c \sqrt{\frac{FkT\Delta f}{P_i}}.$$

ii) *Transmission cavity.* — The loaded Q of the cavity with two couplings is expressed by

$$(2.6) \quad \frac{1}{Q_L} = \frac{1}{Q_0} + \frac{1}{Q_1} + \frac{1}{Q_2},$$

where Q_0 is the unloaded Q , Q_1 the Q of the input coupling and Q_2 the Q of the output coupling. Absorption or emission of power by molecules in the cavity can be represented by

$$\Delta \left(\frac{1}{Q_L} \right) = \frac{1}{Q_m} = \frac{-\Delta P_m}{\omega_0 W},$$

or

$$(2.7) \quad \Delta Q_L = -\frac{Q_L^2}{Q_m}.$$

Here $\omega_0/2\pi$ is the resonant frequency, W the stored energy of the cavity, $-\Delta P_m$ the power absorbed by molecules.

The ratio of the output power P_2 to the input power P_i is

$$\frac{P_2}{P_i} = \frac{1}{Q_1 Q_2} \cdot \frac{1}{(\omega - \omega_0)^2 / \omega_0^2 + 1/4Q_L^2}.$$

At resonance, $\omega = \omega_0$, it becomes

$$(2.8) \quad \frac{P_2}{P_i} = \frac{4Q_L^2}{Q_1 Q_2}.$$

Now the change of output power is calculated from eq. (2.8) and (2.7),

$$\Delta P_2 = P_i \frac{8Q_L}{Q_1 Q_2} \Delta Q_L = -P_2 \frac{2Q_L}{Q_m}.$$

The absorption or emission is detectable when

$$\frac{(\Delta P_2)^2}{16P_2} = P_i \frac{Q_L^4}{Q_m^2 Q_1 Q_2} \geq FkT\Delta f.$$

The sensitivity takes a maximum value when $Q_L^4/(Q_m^2 Q_1 Q_2)$ is maximized. The input and output couplings must be so chosen that

$$(2.9) \quad Q_1 = Q_2 = 2Q_0.$$

In this case the loaded Q is $Q_L = \frac{1}{2}Q_0$, and the minimum detectable absorption can be given by

$$(2.10) \quad \left| \frac{1}{Q_m} \right|_{\min} = \frac{8}{Q_0} \sqrt{\frac{FkT\Delta f}{P_i}}.$$

iii) *Reflection cavity.* - The reflection cavity exhibits some intriguing effects due to interference of input and reflected waves. The reflected power P_1 is given by

$$(2.11) \quad \frac{P_1}{P_i} = \left| \frac{1/Q_1}{i(\omega - \omega_0)/\omega_0 + 1/2Q_L} - 1 \right|^2.$$

At resonance, it becomes

$$(2.12) \quad \frac{P_1}{P_i} = \left(\frac{2Q_L}{Q_1} - 1 \right)^2.$$

When the reflected power is fed to the detector by using a circulator for example, the change of detector power due to the absorption by molecules in

the cavity is

$$\Delta P_1 = -P_i \left(\frac{2Q_L}{Q_1} - 1 \right) \frac{4Q_L^2}{Q_1 Q_m}.$$

More generally, when the reflected wave is mixed with a fraction a of the input wave, the power to the detector at $\omega = \omega_0$ is given by

$$(2.13) \quad \frac{P_d}{P_i} = \left(\frac{2Q_L}{Q_1} - 1 + a \right)^2.$$

The increase of the detector power by the emitted power ΔP_m is obtained from eqs (2.13) and (2.7):

$$(2.14) \quad \frac{\Delta P_d}{P_i} = - \left(\frac{2Q_L}{Q_1} - 1 + a \right) \frac{4Q_L^2}{Q_1 Q_m}.$$

Then the signal power to be compared with noise is

$$\frac{(\Delta P_d)^2}{16P_d} = P_i \frac{Q_L^4}{Q_1^2 Q_m^2},$$

independent of the value of a (*). The factor Q_L^4/Q_1^2 , becomes maximum for a given value of Q_0 , when

$$(2.15) \quad Q_1 = Q_0$$

and hence

$$\frac{1}{Q_L} = \frac{1}{Q_0} + \frac{1}{Q_1} = \frac{2}{Q_0}.$$

Thus the minimum detectable absorption is given by

$$(2.16) \quad \left| \frac{1}{Q_m} \right|_{\min} = \frac{4}{Q_0} \sqrt{\frac{FkT\Delta f}{P_i}}.$$

iv) *Gas absorption coefficient and susceptibility.* — When the molecules in the gas make electric dipole transitions, the dielectric constant of the gas is expressed in a complex form

$$\epsilon = \epsilon' - i\epsilon''.$$

(*) Practically, the value of a should be adjusted so as to deliver an optimum of power level at the detector for maximum sensitivity.

The molecular Q when the gas is filled in a cavity is given by

$$(2.17) \quad \frac{1}{Q_m} = \frac{\varepsilon''}{\varepsilon'} = \frac{\lambda^2}{2\pi\lambda_g} \alpha_g,$$

where α_g is the power absorption coefficient in the waveguide with guide-wavelength λ_g , and $\lambda = 2\pi c/\omega_0$ the free space wavelength.

For magnetic losses, it is customary to express the loss in terms of susceptibility,

$$\chi = \chi' - i\chi'', \quad \mu = 1 + 4\pi\chi.$$

When the magnetic material is partially filled in the cavity, $1/Q_m$ is obtained by assuming that the absorption is weak,

$$(2.18) \quad \frac{1}{Q_m} = \frac{4\pi \int \chi'' H^2 dv}{\int H^2 dv} = 4\pi\eta\chi''.$$

Here η is called the filling factor, and the integration is made over the cavity volume.

It should be noted that both the waveguide spectrometer and cavity spectrometer have nearly equal theoretical limit of sensitivity. Because the unloaded Q of the short-ended waveguide is

$$Q_0 = \frac{2\pi}{\alpha_c \lambda_g},$$

the minimum detectable $1/Q_m$ by the short-ended waveguide spectrometer is

$$\left| \frac{1}{Q_m} \right|_{\min} = 2e \frac{\lambda^2}{\lambda_g^2} \frac{1}{Q_0} \sqrt{\frac{FkT\Delta f}{P_i}},$$

which is approximately equal to (2.10) or (2.16).

v) *Noise figure.* — The noises of vacuum tube amplifiers are fairly well understood. A noise figure of less than 1.5 is obtainable in the megahertz range with a Wallman circuit [2]. Here the noise figure of a microwave spectrometer is discussed. A schematic diagram is shown in Fig. 1. The loss in

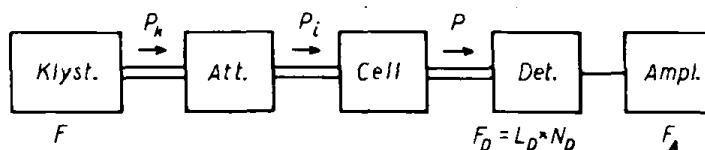


Fig. 1. — Block diagram of a microwave spectrometer.

the attenuator and absorption cell is $L_c = P_K/P$, and L_d is the conversion loss of the detector. The over-all noise figure may be written in the form

$$(2.19) \quad \begin{aligned} F &= \frac{1}{L_c} (F_K - 1) + F_d + L_d(F_A - 1), \\ &= \frac{P}{P_K} (F_K - 1) + L_d(F_A + N_d - 1), \end{aligned}$$

where F_K , $F_d = L_d \cdot N_d$, and F_A are the noise figures of the klystron, detector, and amplifier respectively.

Very few data are available for the noise of reflex klystron oscillators. As a local oscillator in a radar receiver, the *i-f* noise at 30 MHz or 60 MHz is not very large, but it increases for lower beating frequencies. Since the microwave spectrometers are operated with the amplifier at a frequency of 100 kHz or lower, the klystron noise is sometimes quite serious. The following crude theoretical estimate similar to the consideration of maser noise [3] seems useful. If the cavity is assumed to be moderately coupled to the output and the electron beam so that the saturation factor may be taken as 1, the noise power $P_n(f)df$ in the frequency interval from $\nu_0 + f$ to $\nu_0 + f + df$ is calculated approximately

$$(2.20) \quad \frac{P_n(f)df}{P_K} = \frac{Q_L kT df}{\omega_0 W} \left(\frac{2}{\pi}\right)^2 \frac{1}{\tau^2 f^2},$$

where Q_L is the loaded Q of the klystron cavity, T the effective noise temperature of the electron beam, and the correlation time τ is written in terms of the mode number $n + \frac{3}{4}$ and oscillation frequency ν_0 ,

$$\tau = \frac{n + \frac{3}{4}}{\nu_0}.$$

Since $P_K = \omega_0 W/Q_1$, and $Q_1 = 4Q_L$ for optimum coupling of the output and the beam, eq. (2.20) reduces to

$$(2.21) \quad P_n(f) = \frac{kT\nu_0^2}{\pi^2(n + \frac{3}{4})^2} \cdot \frac{1}{f^2}.$$

This gives the noise in a single sideband and agrees with measurements [4] except for the highest mode of pure oscillation. Because of a correlation between fluctuations in the upper and lower sidebands the noise of a klystron employed in the spectrometer as shown in Fig. 1 becomes smaller than the

noise in a single sideband. The effective noise figure of a klystron becomes

$$(2.22) \quad F_K = \frac{P_n(f)}{kT} \frac{2Q_L}{\nu_0} \cdot 2f \div 0.4 \frac{Q_L \nu_0}{(n + \frac{3}{2})^2} \cdot \frac{1}{f},$$

because the derivative of the cavity response function $R(f) = 1/(1 + 2iQ_L f/\nu_0)$ is

$$\frac{dR(f)}{df} = i \frac{2Q_L}{\nu_0}.$$

As a typical example, take $\nu_0 = 2.5 \cdot 10^{10} \text{ s}^{-1}$, $Q_L = 300$, and $n = 5$, and we obtain

$$F_K \div \frac{10^{11}}{f}.$$

The contribution to the over-all noise is

$$(2.23) \quad \frac{F_K - 1}{L_c} \div \frac{10^{11}}{f P_K} P.$$

The above consideration shows that a klystron with larger power gives less noise. A high power klystron operating in a mode with large n is desirable for a high sensitivity spectrometer.

Noise figures of crystal detectors and bolometers for the spectrometer have been discussed by several authors [5-7], and briefly described here in a somewhat different way.

It is true that the noise of a crystal detector increases in proportion to the square of the small dc bias current. However, it seems unreasonable to assume that the noise is proportional to the square of the rectified current when the crystal detector is biased by a small rf signal. Here the noise ratio of the crystal detector is assumed as

$$(2.24) \quad N_x = \frac{C_N P}{f} + 1.$$

The proportionality constant differs from one unit to another, but a typical value for a good detector is

$$C_N = (10^{10} \div 10^{11}) \text{ W}^{-1} \text{ s}^{-1}.$$

The conversion loss of the crystal detector (as a frequency converter) is inversely proportional to the rf power level, when the power is small. It may

be written as

$$(2.25) \quad L_x = \frac{C_L}{P} + L_0,$$

where typical experimental values of the constants are

$$C_L = (10^{-3} \div 10^{-4}) \text{ W}, \quad \text{and} \quad L_0 \approx 3.$$

Then the noise figure of the crystal detector is

$$(2.26) \quad F_x = \frac{C_N L_0}{f} P + \left(\frac{C_L C_N}{f} + L_0 \right) + \frac{C_L}{P}.$$

The noise figure takes a minimum value, when the rf power takes a value,

$$P_{\text{opt}} = \sqrt{\frac{C_L}{C_N} \frac{f}{L_0}} \approx 10^{-7} \sqrt{f}.$$

An example for $f = 100 \text{ MHz}$, gives $P_{\text{opt}} \approx 1 \text{ mW}$ and $F \approx 8$, and another example for $f = 100 \text{ Hz}$, gives $P_{\text{opt}} \approx 1 \mu\text{W}$ and $F \approx 10^5$.

For frequencies $f \leq 10^5 \text{ s}^{-1}$, eq. (2.26) may be expressed approximately

$$F_x \approx \frac{(10^6 \div 10^8)}{f},$$

in a fairly wide range of power level around P_{opt} .

The noise of the following amplifier is usually smaller when a crystal detector is employed. However, when a bolometer or a barretter is employed, the noise figure of the amplifier contributes considerably to the over-all noise figure, since the conversion loss of a bolometer is large.

A theoretical limit of the noise figure of an evacuated bolometer, on the assumption that the bolometer resistance is proportional to the bolometer temperature T_B , and that the heat loss is proportional to $T_B^4 - T^4$, is

$$(2.27) \quad F_B \equiv L_B \cdot N_B = 16 \frac{(P_{\text{dc}} + P_{\text{rf}} + P_{\text{th}})^2}{P_{\text{rf}} P_{\text{dc}}} \cdot \frac{T_B}{T},$$

where P_{dc} , P_{rf} , and P_{th} are the dc power, rf power, and the thermal radiation at the ambient temperature, T . Eq. (2.27) takes a minimum value, $F_{\text{opt}} = 81\sqrt{3}$ when

$$(2.28) \quad P_{\text{dc}} = P_{\text{rf}} = 4P_{\text{th}}$$